Structural Basis of Cytochrome c Presentation by IE^k

Daved H. Fremont,[1] Shaodong Dai,[2] Herbert Chiang,[1]
Frances Crawford,[2] Philippa Marrack,[2,3,4] and John Kappler[2,3,5]

[1]*Department of Pathology and Immunology and Department of Biochemistry and Molecular Biophysics, Washington University School of Medicine, St Louis, MO 63110*
[2]*Howard Hughes Medical Institute, Integrated Department of Immunology, Zuckerman Family/Canyon Ranch Crystallography Laboratory, National Jewish Medical and Research Center, Denver, CO 80206*
[3]*Integrated Department of Immunology,* [4]*Department of Biochemistry and Molecular Genetics, and* [5]*Department of Pharmacology and Program in Biomolecular Structure, University of Colorado Health Science Center, Denver, CO 80262*

Abstract

The COOH-terminal peptides of pigeon and moth cytochrome c, bound to mouse IE^k, are two of the most thoroughly studied T cell antigens. We have solved the crystal structures of the moth peptide and a weak agonist–antagonist variant of the pigeon peptide bound to IE^k. The moth peptide and all other peptides whose structures have been solved bound to IE^k, have a lysine filling the p9 pocket of IE^k. However, the pigeon peptide has an alanine at p9 shifting the lysine to p10. Rather than kinking to place the lysine in the anchor pocket, the pigeon peptide takes the extended course through the binding groove, which is characteristic of all other peptides bound to major histocompatibility complex (MHC) class II. Thus, unlike MHC class I, in which peptides often kink to place optimally anchoring side chains, MHC class II imposes an extended peptide conformation even at the cost of a highly conserved anchor residue. The substitution of Ser for Thr at p8 in the variant pigeon peptide induces no detectable surface change other than the loss of the side chain methyl group, despite the dramatic change in recognition by T cells. Finally, these structures can be used to interpret the many published mutational studies of these ligands and the T cell receptors that recognize them.

Key words: T cell receptor • X-ray crystallography • antigen presentation • peptide • cytochrome

Introduction

One of the most heavily studied antigenic peptides in mice comes from the COOH-terminal end of pigeon cytochrome c (PCC),* encompassing amino acids 89–103 (peptide derived from the COOH terminus of PCC [pPCC]). This peptide contains the dominant pigeon cytochrome c epitope for $CD4^+$ T cells in many strains of mice (1). Over the years, many immunological principles have been defined and studied using this peptide and its homologues from the cytochrome c's of other species, especially the equivalent peptide from moth cytochrome c (pMCC).

In H-2^k or H-2^a mice, the IE^k MHC class II molecule (MHCII) presents pPCC and pMCC to T cells. The phenomenology associated with the response to these peptides led to the discovery of two complementing "immune response" genes that later turned out to be the structural genes for the α and β chains of the IE^k molecule (2). Mutational studies have predicted which of the pPCC and pMCC amino acid side chains are important for the binding of the peptides to the IE^k molecule (3, 4). An important difference between pMCC and pPCC is the fact that pPCC has an Ala inserted at amino acid 103. This insertion causes pPCC to raise a "heteroclitic" response to the pMCC, which means that although pPCC and pMCC are virtually completely cross reactive, essentially all T cell clones raised by immunization with pPCC respond better to pMCC (5). The data have suggested that this phenomenon is linked to the interaction of the peptide with the MHC molecule rather than the αβTCR, but the structural basis of this difference has remained unknown (6).

Address correspondence to John W. Kappler, Howard Hughes Medical Institute, National Jewish Medical and Research Center, 1400 Jackson Street, Denver, CO 80206. Phone: 303-398-1322; Fax: 303-398-1396; E-mail: kapplerj@njc.org

**Abbreviations used in this paper:* CPK, Corey, Pauling, Koltan; MHCI, MHC class I; MHCII, MHC class II; pMCC, peptide derived from the c-terminus of moth cytochrome c; PCC, pigeon cytochrome c; pPCC, peptide derived from the COOH terminus of pigeon cytochrome c.

 J. Exp. Med. © The Rockefeller University Press • 0022-1007/2002/04/1043/10 $5.00
Volume 195, Number 8, April 15, 2002 1043–1052
http://www.jem.org/cgi/doi/10.1084/jem.20011971

The repertoire of αβTCR expressed by T cells responding to pPCC and pMCC is dominated by receptors bearing AV11S1 and AV11S2 (Vα11.1 and Vα11.2, respectively) and BV3S1 (Vβ3) (7). Many Vα11/Vβ3$^+$ T cell clones/hybridomas specific for these peptides are in widespread use (8–10) and the genes for the αβTCRs of a number of these clones have been used to produce αβTCR-transgenic mice (11–14). These mice, as well as those transgenic for various versions of the IE^k molecule (15, 16), have been used over the years to study the principles of T cell activation as well as positive and negative selection in the thymus. The interaction of αβTCRs with IE^k/pPCC or IE^k/pMCC has been extensively studied both in vitro and in vivo. These studies have predicted which of the αβTCR, IE^k, and peptide amino acids are important in the interaction (4, 6, 17–21).

pPCC and pMCC have also been used to study the phenomenon of antagonism. Amino acid variants of a number of antigenic peptides have been identified, which not only fail to stimulate particular T cell clones or hybridomas that had been raised to the wild-type peptide, but also render the T cell unresponsive to a subsequent or simultaneous challenge with the wild-type peptide (22). Although the mechanism of this phenomenon is not fully understood, it has been shown to involve some type of aberrant or incomplete receptor signaling that effectively desensitizes the receptor to subsequent ligation. In the case of pPCC and pMCC, several clones were antagonized by variant peptides bearing only slight differences from the wild-type peptides (23, 24)

In the current study, we have solved the crystal structure of the IE^k molecule in complex with either pMCC or pPCC bearing a single amino acid change (Thr to Ser at amino acid 102) that renders it either a poor agonist or an antagonist for many T cell clones. The structures reveal the basis for the differences between pMCC and pPCC in binding to IE^k. They also show that the Thr to Ser change results in only a very minor surface difference between the two molecules. Finally, the structures support many of the predictions made in previous studies concerning contacts between the peptides and either the IE^k molecule or the T cell receptor.

Materials and Methods

IE^k–pMCC and IE^k–pPCC(T102S). The expression, production, and purification of soluble IE^k with covalently attached peptides have been previously described (25–27). In this study two different peptides were used: pMCC, RDLIAYLKQATK, corresponding to amino acids 92–103 of moth cytochrome c, and pPCC(T102S), RDLIAYLKQASAK, corresponding to amino acids 92–104 of pigeon cytochrome c, with the exception that the Thr at amino acid 102 was changed to Ser. In discussing the structure of individual peptide amino acids when bound to IE^k, we use the convention of designating the first peptide anchor amino acid as p1 and number the other amino acids accordingly, e.g., p9Lys or p9K. IE^k amino acids are designated by chain and number, e.g., β9Glu or α66Asp. Also, for simplicity, MHCII covalent peptide complexes are referred to with a (–) connecting the MHC and peptide name, e.g., IE^k–pMCC, whereas noncovalent complexes use a (/), e.g., IE^k/pMCC.

Crystallization. Both IE^k–pMCC and IE^k–pPCC(T102S) were crystallized by the hanging drop method. IE^k–pMCC crystals were grown in 1-μl drops containing ~11 mg/ml of protein, 12% PEG-4000, 12% 2-propanol, and 60 mM of sodium acetate buffer at pH 5.5. IE^k–pPCC(T102S) crystals were grown in 1-μl drops containing ~10 mg/ml of protein, 14% PEG-4000, 14% 2-propanol, 1.4% ethylene glycol, 70 mM of sodium acetate buffer at pH 5.0, and 320 mM of ammonium sulfate.

Data Collection. IE^k–pMCC and IE^k–pPCC(T102S) crystals were cryopreserved by briefly soaking in mother liquor with the addition of 20% ethylene glycol and 10% glycerol followed by rapid cooling in a gaseous stream of nitrogen at 100°K (Oxford Cryosystems). Diffraction data for a single IE^k–pMCC crystal were collected in the X4A beamline at the National Synchrotron Light Source at Brookhaven National Laboratory using a wavelength of 0.9795 Å and PhosphorImager plates with 2° oscillations. Data were processed with Denzo and scaled/merged with SCALEPACK (HKL Research, Inc.; reference 28). Diffraction data for a single IE^k–pPCC(T102S) crystal were collected in the crystallography facility at the Howard Hughes Medical Institute using a wavelength of 1.54 Å, a Rigaku rotating anode generator, Yale mirrors, and a RAXIS IV detector with 1° oscillations. Data were processed, scaled, and merged using the BIOTEX program (Molecular Structure Corp.). Both of the crystals were of space group C2 with similar dimensions and packing, and both had two molecules in the asymmetric unit. Details of the collection and processing statistics are in Table I.

Structure Determination. The structures of IE^k–pMCC and IE^k–pPCC(T102S) were solved by molecular replacement using the program AMoRe (29, 30). The search model was the IE^k–pHB structure with the peptide and linker removed (31). The very low resolution data (>10 Å) from the IE^k–pPCC(T102S) dataset were omitted due to problems with saturation. The initial models were improved with rigid body refinement using the program Xplor/CNS (32). Multiple rounds of refinement with Xplor/CNS and model building with oxygen (33) were used to improve the model when the peptides were added. The final model of IE^k–pMCC had 792 amino acids and that of IE^k–pPCC(T102S) had 794 amino acids. As in the case of the other IE^k structures that we have solved, relatively weak electron density was seen for most of the linker attaching the peptide to the β chain NH_2 terminus, and for the loop connecting the first and second β strands of the β2 domain. In the later stages of refinement, the following *N*-acetyl glucosamines were added to some asparagines based on positive electron density in Fo-Fc maps: six to the IE^k–pMCC structure and four to the IE^k–pPCC(T102s) structure. In addition, the following water molecules were added: 215 to the IE^k–pMCC structure and 317 to the IE^k–pPCC(T102s) structure. Refinement and final model statistics are listed in Table I. For figures, average structures were calculated for both molecules from the two molecules in the asymmetric units using the programs MOLEMAN and AVEPDB (34, 35). Coordinates have been submitted to the Protein Data Bank (available at http://www.rcsb.org/pdb/ under accession numbers 1KT2 and 1KTD).

Results and Discussion

The Peptide Motif for Binding to IE^k. In previous studies (31, 36), we reported that the structure of the IE^k molecule

Table I. *Data Collection and Refinement Statistics*

Data collection	pMCC	pPCC(T102S)
Space group	C2	C2
Unit cell dimensions (Å)	a = 147.8, b = 56.9, c = 116.0	a = 145.5, b = 57.3, c = 116.6
Unit cell angles (°)	β = 92.1	β = 94.2
No. of molecules in AU	2	2
Resolution limits (Å)	20-2.8 (2.95-2.80)[a]	100-2.4 (2.56-2.40)
Unique reflections	22,827 (3,185)	36,433 (5,970)
Completeness (%)	95.2 (93.4)	95.2 (90.2)
Averave redundancy	2.5	3.1
Average I/σ	11.1 (2.4)	16.8 (2.8)
R_{merge} (%)[b]	9.7 (31.7)	4.7 (26.4)
Refinement		
Resolution (Å)	20-2.8 (2.89-2.80)	10-2.4 (2.5-2.4)
Rejection criterion	F ≤ 0	F ≤ 0
Total reflections	22,378 (1,845)	35,965 (3,773)
Reflections used for Rfree	1,088 (85)	1,785 (191)
Rworking[c] (%)	22.1 (32.2)	22.0 (31.3)
Rfree[c] (%)	29.3 (42.2)	27.9 (36.4)
Average B factors (Å^2)	47.9	48.8
Ramachandran data		
Percentage of residues in:		
Favored regions	85.7	88.0
Allowed regions	13.3	10.9
Generously allowed regions	0.8	0.9
Disallowed regions	0.3	0.1
Rmsd		
Bonds (Å)	0.0069	0.0064
Angles (°)	1.397	1.288
Bfactor main chain (1.5)[e] (Å^2)	1.95	1.31
Bfactor side chain (2.0)[e] (Å^2)	1.45	1.39
Cross-validated coord. error (Å)	0.47	0.41

[a]All data (outer shell).
[b]Rmerge = $\Sigma(|I - \langle I \rangle|)/\Sigma(I)$.
[c]Rworking/free = $\Sigma||F_o| - |F_c||/\Sigma|F_o|$.
[d]Excluding Gly and Pro.
[e]Target value.

bound to two different peptides: pHB, a highly immunogenic peptide derived from an allele of the β chain of mouse hemoglobin and pHSP, a peptide derived from HSP70, which is a major self-peptide that occupies natural IE^k. These structures revealed four anchor residues in each peptide interacting with four pockets in the IE^k peptide binding groove (Fig. 1 A). The very hydrophobic p1 pocket accepted amino acids with aliphatic side chains (Ile in pHB and Val in pHSP). The large, somewhat hydrophobic p4 pocket was filled with a Phe in both cases. The very hydrophilic p6 pocket contained a Glu in the case of pHB. The carboxylate of this amino acid participated in an extensive hydrogen bonding network that included two IE^k acidic amino acids (α11Glu and α66Asp). In the case of pHSP, the Ala at this position only filled the very top of the pocket, with an extra water molecule now maintaining the hydrogen bonding network. Finally, the p9 pocket of IE^k consisted of a long tunnel culminating in a negatively charged β9Glu that formed a salt bridge with the ε amino group of a p9Lys at that position in both peptides.

This structural information, as well as other published data (1, 4, 37–45), were used to align and predict the anchor residues of pMCC and pPCC(T102S), as well as other peptides that are the dominant IE^k epitopes in for-

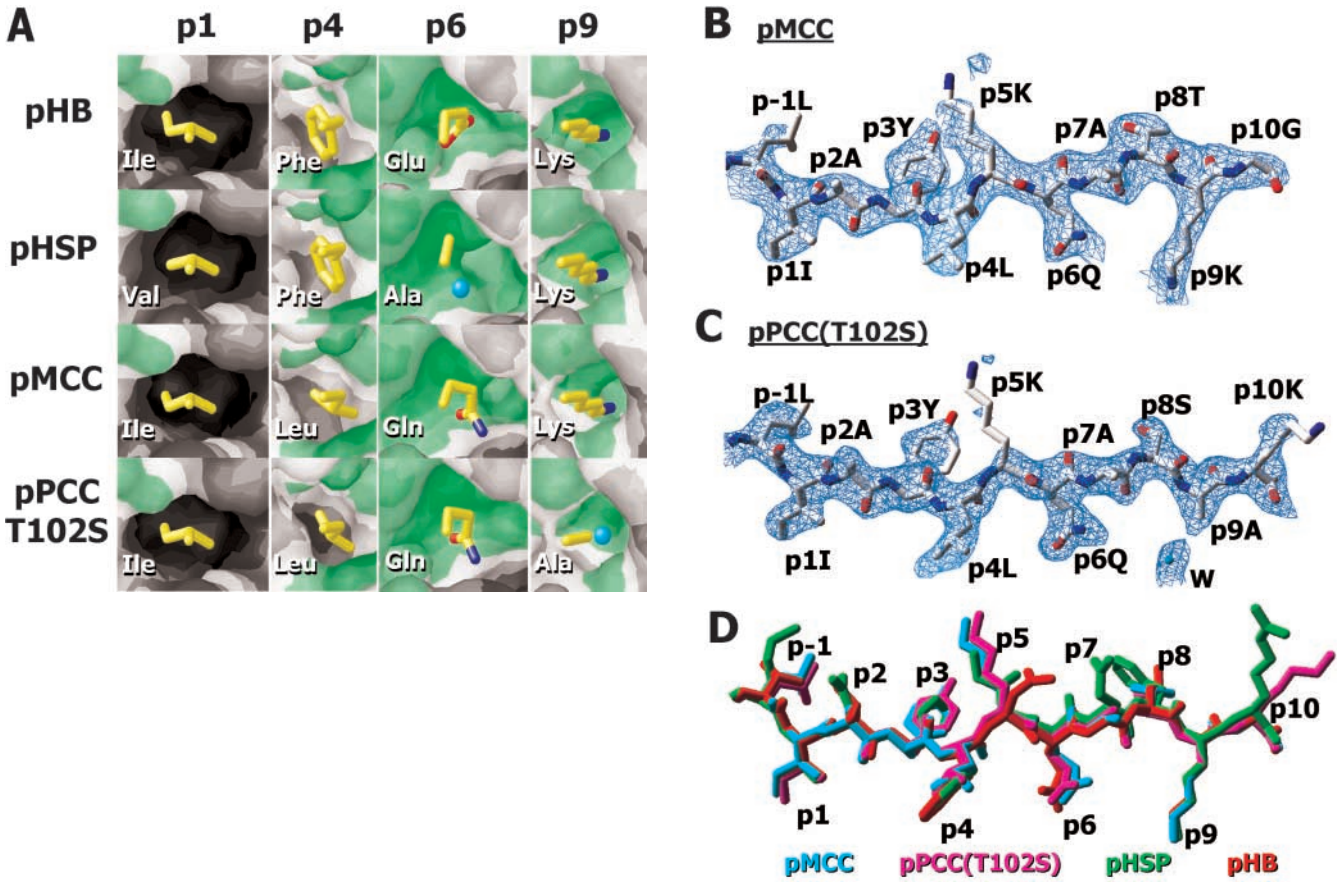

Figure 1. Structure of pMCC and pPCC(T102S) bound to IE^k. (A) Solvent-accessible surface (probe radius of 1.4 Å) representation of the four peptide amino acid binding pockets (p1, p4, p6, and p9) of IE^k with the side chains of four bound peptides are shown. IE^k surface colored by relative hydrophobicity (Gilliard scale). Gray, hydrophobic; white, neutral; green, hydrophilic. Peptide side chains are shown as wire frame. Yellow, carbon; blue, nitrogen; red, oxygen; cyan, water. The figure was made with Protein Explorer (http://proteinexplorer.org). (B) Peptide/water omit electron density map (Fo-Fc, 2.5σ) surrounding pMCC from p1 to p11. The figure was made with the Swiss PDBViewer. (C) This shows the same as panel B for pPCC(T102S), and also shows the electron density for an extra water molecule (W) in the p9 pocket. (D) Overlay of four peptides from IE^k structures. Cyan, pMCC; magenta, pPCC(T102S); green, pHSP; red, pHB. The structures were superimposed via the backbones of the α1 and β1 domains using Swiss PDBViewer. The figure was made with the Swiss PDB Viewer.

eign protein antigens, or major self-peptides isolated from IE^k naturally present on the surface of B cells, and thymic epithelium in unimmunized mice (Fig. 2). This alignment predicts an aliphatic amino acid at the p1 position. The p4 pocket is predicted to be more forgiving, preferring hydrophobic amino acids such as Phe and Leu, but also allowing other amino acids. The p6 pocket appears to have a preference for amino acids that can participate in the hydrogen bonding network underlying the peptide (Glu, Gln, and Asn), but small side chains such as the Ala in pHSP are also allowed. The p9 pocket is predicted almost invariably to be Lys.

Using this alignment, the p1, p4, and p6 pockets of IE^k were predicted to contain Ile, Leu, and Gln, respectively, for both pMCC and pPCC(T102S). Although the p9 amino acid was predicted to be Lys for pMCC, two possibilities existed for pPCC(T102S). pPCC(T102S) has an Ala insertion at p9 that shifts the Lys to p10. Therefore, either the Ala must now occupy the p9 pocket or the peptide backbone must kink to allow the shifted Lys side chain to remain in the p9 pocket. In either case, the adjustments to the Ala insertion might contribute to poorer binding by pPCC to IE^k.

Interactions of pMCC and pPCCT102S with IE^k. To test these predictions, we solved the crystal structures of IE^k bound to pMCC and pPCC(T102S) by molecular replacement to resolutions of 2.8 and 2.4 Å, respectively, using the high resolution IE^k–pHB structure with the peptide removed as a search model. In the final models, the backbones of the IE^k portions of the structures were virtually identical to that of the IE^k in the IE^k–pHB structure. For example, using the program Swiss PDBViewer (46) to compare the combined α1/β1 domains, the RMSD's were 0.28 Å for backbone atoms and 0.54 Å for all atoms comparing IE^k–pMCC to IE^k–pHB. Comparing IE^k–pPCC(T102S) to IE^k–pHB, the values were 0.32 and 0.51 Å, respectively. Peptide omit electron density maps clearly showed the peptides in the binding groove (Fig. 1, B and C) and in the final models, the paths of the peptides through the binding grooves were nearly identical to those seen with IE^k–pHB and IE^k–pHSP (Fig. 1 D).

Peptide Motif for Binding to IE^k

Source	aa Nos.	Sequence									
HB	(68-76)	I	T	A	F	N	E	G	L	K	
HSP	(238-246)	V	N	H	F	I	A	E	F	K	
MCC	(95-103)	I	A	Y	L	K	Q	A	T	K	
PCC	(95-104)	I	A	Y	L	K	Q	A	T	A	K
PCC	(T102S)	I	A	Y	L	K	Q	A	S	A	K
HEL	(88-96)	I	T	A	S	V	N	C	A	K	
SWMb	(69-77)	L	T	A	L	G	A	I	L	K	
λrep	(18-26)	L	K	A	I	Y	E	K	K	K	
OVA	(255-263)	L	E	S	I	I	N	F	E	K	
Snase	(89-97)	L	A	Y	I	Y	A	D	G	K	
LLO	(218-226)	I	A	K	F	G	T	A	F	K	
FluHA	(246-254)	I	S	I	Y	W	T	I	V	K	
HIV	(424-432)	I	N	M	W	Q	E	V	G	K	
Moβ2m	(37-45)	I	Q	M	L	K	N	G	K	K	
MoCCinh	(45-53)	I	Q	N	A	V	Q	G	V	K	
MoSA	(351-359)	V	E	A	A	R	N	L	G	R	
MoER60	(448-461)	I	Y	F	S	P	A	N	K	K	
Relative	Position (p)	1	2	3	4	5	6	7	8	9	10

Figure 2. Peptide motif for binding to IE^k. The core sequences of pHB and pHSP are aligned based on their solved structures bound to IE^k, with the positions of the four anchor residues (p1, p4, p6, and p9) highlighted. A series of other IE^k binding peptides that were either identified as the major epitopes from foreign antigens or self-peptides isolated from IE^k, were aligned based on the predicted occupancy of the four binding pockets with particular weight on p1 and p9. Only the central regions of the peptides are shown. Abbreviations and references: HB, mouse hemoglobin (37); HSP, mouse heat shock protein 70, (38); MCC, moth cytochrome c (1); PCC, pigeon cytochrome c (1); HEL, hen egg lysozyme (39); SWMb, sperm whale myoglobin (40); λrep, λ repressor (39); OVA (255–263), chicken ovalbumin (4); Snase, staphylococcal nuclease (41); LLO, listeriolysin O (42); FluHA, influenza hemagglutinin (43); HIV, HIV gp120 (44); Moβ2m, mouse β2 microglobulin (38); MoCCinh, mouse cytochrome c inhibitor (38); MSA, mouse serum albumin (38); ER60, mouse ER-60 protease (45).

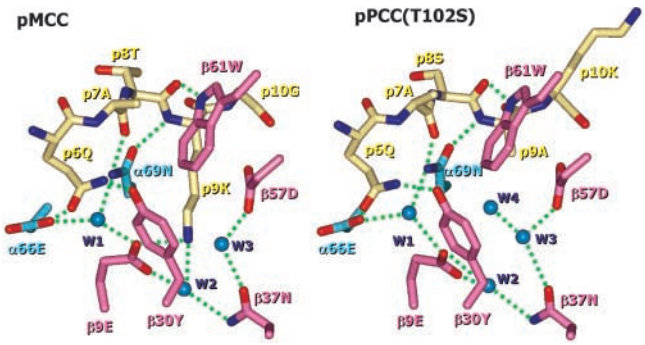

Figure 3. Details of the p6 and p9 pockets of IE^k–pMCC and IE^k–pPCC(T102S). Shown are wire frame representations of residues p6-p10 of pMCC (left) and pPCC(T102S) (right). Also shown for both molecules are side chains of α66Asn, α69Asn, β9Glu, β30Tyr, β37Asn, β57Asp, and β61Trp. Light yellow, peptide carbon; cyan, α chain carbon; magenta, β chain carbon; blue, nitrogen; red, oxygen. Three water molecules (W1–W3) common to both molecules are shown as well as a water molecule (W4) that is unique to the IE^k–pPCC(T102S) structure (light blue). Some of the predicted hydrogen bonds among the atoms are shown as green dotted lines. Figures were made with WebLab ViewerPro (Accelrys c.).

The structure of pMCC bound to IE^k confirmed the MHCII binding motif prediction (Fig. 1, A, B, and D). Side chains from four amino acids, Ile at p1, Leu at p4, Gln at p6, and Lys at p9, filled the four IE^k pockets. Amino acids at positions p1, p6, and p9, but not at p4, were predicted by mutagenesis experiments to be important in the interaction of pMCC with IE^k (4). In these experiments virtually any amino acid could be substituted at the p4 position without penalty. These results suggest great flexibility in this large pocket in accepting amino acid side chains and relatively little contribution from the side chain to the overall energy of pMCC binding.

As expected, the pPCC(T102S) peptide bound to IE^k (Fig. 1, A, C, and D) also has the Ile at p1, Leu at p4, and Gln at p6, all in conformations very similar to those in pMCC. The structure also clearly shows the adjustment to the inserted Ala at the p9 position of the peptide. Although the side chain of the Lys at p9 of pMCC points down into the pocket, this position is occupied by the inserted Ala whose methyl side chain only fills the very top of the pocket, whereas the p10 Lys is shifted and rotated so that the side chain is now completely solvent-exposed. An extra water molecule is now found in the p9 pocket. This suggests that the loss of the buried Lys side chain is most likely a major reason for the weaker binding of pPCC compared with pMCC.

Details of the peptide interactions with IE^k in the region of the p6 and p9 pockets are shown in Fig. 3. The side chain of the p9Lys of pMCC extends through a hydrophobic tunnel to a salt bridge with β9Glu and interacts with a water molecule (W2). Other interactions at this end of the peptide include the highly conserved hydrogen bonds between β61Trp and α69Asn, the peptide backbone seen in nearly all MHCII structures, and an extensive hydrogen bond network that includes p6Gln, α66Glu, β30Tyr, and several water molecules. In the IE^k–pPCC(T102S) structure, the interactions at p9 are lost and the pocket is partially filled with an extra water molecule (W4). However, the other details of the hydrogen bonding network are preserved.

The main chain of pPCC(T102S) has not kinked to maintain a Lys in the p9 pocket, but rather its path through the binding groove is identical to that of pMCC. Kinks in peptides bound to MHC class I (MHCI) are common (47, 48) and function to maintain the conserved binding of MHCI to the peptide NH_2 and COOH termini, and allow the insertion of favorable amino acid side chains in the MHCI binding pockets. However, in all solved structures of MHCII, including those presented here, the peptide takes a very similar, nearly linear course through the binding groove, held in place by hydrogen bonding between its backbone and the side chains of conserved amino acids on the MHC α helices (31, 49–53).

It is difficult to predict the net changes in the IE^k–pPCC(T102S) structure if the peptide were to be kinked and rotated to preserve a Lys in the p9 pocket. The van der Waals interactions with the Lys side chain as well as the salt bridge and the hydrogen bonds to its ε-amino group, would be gained. However, it is likely that the conserved peptide backbone interactions with β61Trp and α69Asn would be lost. Also, depending on the precise nature of the kink, the hydrogen bonding network involving the p6Gln might be disturbed. Apparently, the energy gained by the new interactions would not compensate for the loss of these other interactions.

Peptide Amino Acids Interacting with αβTCRs. The interaction of IE^k/pMCC and IE^k/pPCC with the αβTCRs of many different T cell clones has been extensively studied. Various mutagenesis experiments have shown that the amino acids at p2, p3, p5, p7, and p8 are involved in recog-

nition by various T cell clones (4, 6). These represent all of the surface-exposed amino acids in the center of the bound peptides (Fig. 4 A). Of these, the p5Lys has been shown to be the most important. For most T cell clones raised by immunization with pMCC or pPCC, effective stimulation is critically dependent on a Lys at this position. This Lys is directly in the center of the binding pocket with its side chain pointing up and out of the groove into the solvent.

T cell recognition of these peptides is also usually very dependent on the p8Thr. Substitution of any other amino acid at this position, even the conserved Thr to Ser substitution shown here, often compromises T cell activation. For the Thr to Ser change, the peptide is converted to a weaker agonist in that equivalent T cell activation now requires more peptide (4, 24). For one T cell clone, partial blocking of the function of CD4 with a monoclonal antibody converted this mutant peptide to an antagonist, i.e., exposure of the clone to the p8Ser peptide under these conditions inhibited its response to the wild-type peptide (54). Another mutation at this position (Thr to Gly) has also been shown to produce an even more antagonistic peptide (24).

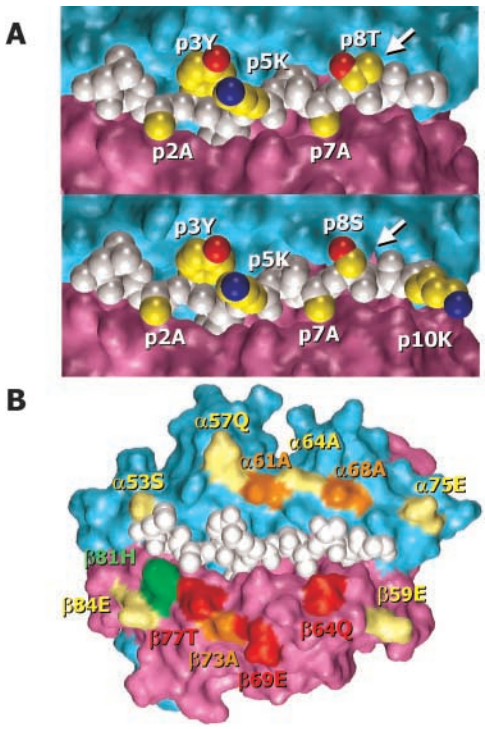

Figure 4. Surface amino acids of IE^k–pMCC and IE^k–pPCC(T102S) that are important for αβTCR recognition. (A) A portion of the solvent-accessible surfaces of the α1 and β1 domains of IE^k–pMCC (top) and IE^k–pPCC(T102S) (bottom) are shown. Cyan, α chain; magenta, β chain. A van der Waal's Corey, Pauling, Koltan (CPK) representation of the peptide is shown from p1 to p10. The peptide atoms are white except for the side chains of the five central surface exposed amino acids and the Lys at p10 of pPCC(T102S). These are colored by atom type. Yellow, carbon; blue, nitrogen; red, oxygen. The methyl group of the p8Thr of pMCC and its absence on the p8Ser of pPCC(T102S) are indicated with white arrows. The figure was made with WebLab ViewerPro. (B) The solvent-accessible surfaces of the α1 and β1 domains of IE^k–pMCC are shown. A van der Waal's CPK representation of the peptide is shown from p1 to p10 in white. Except for the 13 amino acids mutated in the study by Jorgensen et al. (20), the IE^k α chain is colored cyan and the β chain is colored magenta. The other 13 amino acids are colored according to the effects of their mutation. Red, the response of at least three out of four T cell hybridomas compromised by mutation; orange, the response of only one out of four T cell hybridomas compromised by mutation; green, the response of one hybridoma improved by mutation; yellow, no effect of mutation. The figure was made with WebLab ViewerPro.

In the region of p8, the only detectable surface structure alteration induced by the Thr to Ser substitution was the loss of the Thr side chain methyl group (Fig. 3 and Fig. 4 A). The Cβ carbons and hydroxyl oxygens appear to be in identical positions in both structures. The backbone of the peptide and the position of the other amino acid side chains in this region did not change significantly. Therefore, either this methyl group is an essential contact point for the αβTCR or, less likely, its loss confers some kinetic instability to this region of the molecule that is not revealed by this static structure. As previously described, the insertion of an Ala at p9 of pPCC(T102S) has forced the Lys at p10 out of its binding pocket and onto the molecule surface. This alteration does not seem to be detected by most T cell clones, which suggests that the αβTCR does not usually contact this area of the surface.

The requirements for some of the other solvent-exposed peptide amino acids are not quite as stringent for recognition by T cell clones. For example, several receptors accept an Ala to Gly substitution at p2 or p7, but for the most part larger amino acids are not tolerated, perhaps because of steric problems rather than essential receptor–Ala contacts. Phe, or sometimes Trp but not Leu or Met, is accepted in place of the p3Tyr, which suggests that an aromatic amino acid may be essential at this position. In both of our structures, the close proximity of the Tyr aromatic ring to the side chain of the p5Lys may indicate a role for this interaction in positioning this crucial Lys for αβTCR recognition. This interaction has been suggested by nuclear magnetic resonance studies (55).

IE^k Amino Acids Interacting with αβTCRs. A mutational study of IE^k revealed a number of amino acids on the α and β chain α helices that were important for the recognition of the IE^k–pMCC complex by T cells (21). In these experiments, single mutations were introduced into the IE^k molecule at six positions of the α chain (α53Ser to Asn, α57Gln to Arg, α61Ala to Val, α64Ala to Val, α68Ala to Val, and α75Glu to Lys) and seven positions of the β chain (β59Glu to Lys, β64Gln to Arg, β69Glu to Lys, β73Ala to Val, β77Thr to Gln, β81His to Tyr, and β84Glu to Lys). Although no IE^k structure was available at the time, the authors predicted that these amino acids would lie on the top of the α helices based on sequence homology to MHCI (56). The IE^k structures show that this prediction was indeed correct (Fig. 4 B).

Each mutated IE^k molecule was expressed at the cell surface and tested for binding and presentation of the pMCC to four different T cell hybridomas. In general, the α chain mutations had less effect than those on the β chain, although several of the α chain substitutions were quite con-

servative (Ala to Val). These amino acids are colored on the surface of the IE^k molecule (Fig. 4 B) according to the effect of these mutations. Several of the mutations (β64Gln to Arg, β69Glu to Lys, and β77Thr to Gln) severely reduced the response of at least three of the hybridomas (red). Others (α61Ala to Val, α68Ala to Val, and β73Ala to Val) compromised the response of only one of the four hybridomas (orange). Mutation of β81His to Tyr (green) had no effect on three of the hybridomas, but greatly enhanced the response of the fourth. Mutations at the other positions, which were mainly at the extremities of the α helices, had no effect on T cell recognition (yellow). In total, these data suggest that the main sites of αβTCR interaction with this MHCII peptide ligand are clustered on the upward face of the complex and focused on central peptide residues and the tops of the arched α helices.

Predicted αβTCR Interactions with pMCC and pPCC. Several studies have investigated αβTCR amino acids important in IE^k–pMCC and IE^k–pPCC recognition. For example, experiments have been performed using pMCC and variants at position p5 and p8 to immunize mice bearing a transgene encoding either the α or β chain of an αβTCR from an IE^k/pMCC–reactive T cell (20). Thus, the responding T cells had one of the αβTCR chains fixed by the transgene, whereas the other was allowed to vary. From the sequences of the CDR3s of the varying αβTCR chain, the authors argued convincingly that the p5Lys interacted with a conserved Glu at position 94 of VαCDR3, whereas the p8Thr interacted with a conserved Asn at position 97 of VβCDR3.

These two alleles of Vβ3 have been identified in mice: Vβ3a and Vβ3b (BV3S1A1 and BV3S1A2, respectively). These differ only at amino acid 31 in what is predicted to be the Vβ3 CDR1. This amino acid is Val in Vβ3a and Phe in Vβ3b. Vβ3 dominates the response to pPCC or pMCC in mouse strains that carry Vβ3a, but not in those with Vβ3b (57). Furthermore, direct mutation of amino acid 31 from Val to Phe in the receptor of a Vβ3a bearing IE^k/pMCC–reactive T cell hybridoma eliminated IE^k/pMCC recognition (10). These findings suggest a critical interaction between the Vβ3 CDR1 loop and the IE^k–pMCC and IE^k–pPCC ligand, which is disrupted by the Val to Phe substitution.

There are no crystal structures of αβTCRs bound to IE^k peptide. However, it is reasonable to hypothesize that the orientation of an αβTCR bound to IE^k will be similar to those seen in crystal structures of other αβTCR complexes with MHCI and MHCII ligands (58–63). In these structures, the αβTCR sits diagonally on the top of the MHC molecule, wedged between the arches of the MHC α helices with the Vα, and Vβ CDR3s are centered over the middle of the peptide. So far, in all cases the orientation of the αβTCR has been similar with Vα on the peptide NH_2-terminal side and the Vβ on the peptide COOH-terminal side. Within these constraints, however, the various αβTCRs swivel by up to 35°.

Therefore, in order to interpret some of these findings we superimposed IE^k–pMCC on the MHCII portion of two solved αβTCR–MHCII peptide complexes (61, 62) to predict how the CDRs of an anti–IE^k/pMCC αβTCR might sit on the ligand (Fig. 5 A and B). These models strongly support the results of the mutational studies. The Vα and Vβ CDR3 loops (cyan) are predicted to lie directly over the center of the pMCC peptide. The side chain of p5Lys is in close proximity to the predicted positions of the Vα94, and the side chain of p8Thr is in close proximity to the predicted positions of the Vβ97. It is easy to see how mutations in either one of these peptide amino acids might alter the αβTCR binding kinetics and affinity. The predicted position of Vβ31 in Vβ CDR1 is such that a substitution of Phe for Val at this position would probably interfere with the interaction of VβCDR1 with the α helix of the IE^k α chain. The seven amino acids of IE^k that affect αβTCR interaction when mutated all lie in positions close to the αβTCR CDR loops. Overall, this model agrees remarkably with the published biochemical and mutational studies.

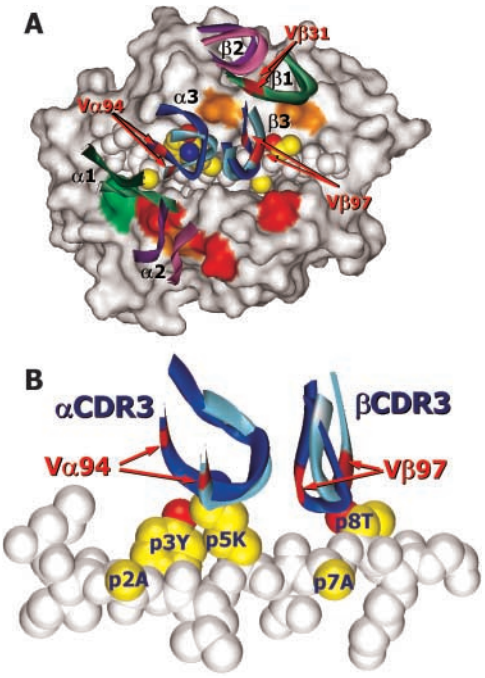

Figure 5. Predicted T cell receptor interactions with IE^k/pMCC. (A) Top view of the solvent-accessible surface of the α1 and β1 domains of IE^k–pMCC are colored white except for α61, α68, β64, β69, β73, β77, and β81, which are colored as in Fig. 4 B. A van der Waal's CPK representation of the peptide is shown from p1 to p10 and is colored as in Fig. 4 A. Two αβTCRs, one from HA1.7 (specific for DR1 plus a peptide from influenza hemagglutinin) (64) and the second from D10 (specific for IA^k plus a peptide from conalbumin) (65), whose structures were solved bound to their MHCII peptide ligands (61, 62), were aligned on the IE^k–pMCC structure by superimposing the backbones of the MHC molecule α1 and β1 domains. Ribbons, the Vα and Vβ CDR loops (α1, α2, α3, β1, β2, and β3) of the two αβTCRs; dark green, HA1.7 αβTCR Vα/β CDR1; purple, Vα/β CDR2; blue, Vα/β CDR3; light green, D10 αβTCR Vα/β CDR1; magenta, Vα/β CDR2; cyan, Vα/β CDR3. The positions of three αβTCR amino acids, Vα94, Vβ31, and Vβ97, are labeled and colored red. (B) Side view of the peptide and CDR3 portions of Fig. 4 A with other parts of the molecules removed. The figures were made with WebLab ViewerPro.

We wish to thank J. Clements for technical assistance. Coordinates have been submitted to the Protein Data Bank (available at http://www.rcsb.org/pdb/ under accession numbers 1KT2 and 1KTD).

This work was supported in part by USPHS grants AI-17134, AI-18785, and AI-22295. D.H. Fremont was partially supported by Burroughs-Wellcome Fund and the Kilo Foundation during the course of this work.

Submitted: 26 November 2001
Revised: 28 February 2002
Accepted: 11 March 2002

References

1. Heber-Katz, E., R.H. Schwartz, L.A. Matis, C. Hannum, T. Fairwell, E. Appella, and D. Hansburg. 1982. Contribution of antigen-presenting cell major histocompatibility complex gene products to the specificity of antigen-induced T cell activation. *J. Exp. Med.* 155:1086–1099.
2. Schwartz, R.H., A.M. Solinger, M. Ultee, and E. Margoliash. 1978. Genetic control of the T-lymphocyte proliferative response to cytochrome c. *Adv. Exp. Med. Biol.* 98:371–386.
3. Fox, B.S., C. Chen, E. Fraga, C.A. French, B. Singh, and R.H. Schwartz. 1987. Functionally distinct agretopic and epitopic sites. Analysis of the dominant T cell determinant of moth and pigeon cytochromes c with the use of synthetic peptide antigens. *J. Immunol.* 139:1578–1588.
4. Reay, P.A., R.M. Kantor, and M.M. Davis. 1994. Use of global amino acid replacements to define the requirements for MHC binding and T cell recognition of moth cytochrome c (93–103). *J. Immunol.* 152:3946–3957.
5. Solinger, A.M., M.E. Ultee, E. Margoliash, and R.H. Schwartz. 1979. T lymphocyte response to cytochrome c. I. Demonstration of a T cell heteroclitic proliferative response and identification of a topographic antigenic determinant on pigeon cytochrome c whose immune recognition requires two complementing major histocompatibility complex-linked immune response genes. *J. Exp. Med.* 150:830–848.
6. Hansburg, D., T. Fairwell, R.H. Schwartz, and E. Appella. 1983. The T lymphocyte response to cytochrome c. IV. Distinguishable sites on a peptide antigen which affect antigenic strength and memory. *J. Immunol.* 131:319–324.
7. Sorger, S.B., L.A. Matis, I. Engel, D.L. McElligott, P.J. Fink, and S.M. Hedrick. 1988. The influence of MHC gene products on the generation of an antigen-specific T-cell repertoire. *Ann. N. Y. Acad. Sci.* 532:18–32.
8. Hedrick, S.M., L.A. Matis, T.T. Hecht, L.E. Samelson, D.L. Longo, E. Heber-Katz, and R.H. Schwartz. 1982. The fine specificity of antigen and Ia determinant recognition by T cell hybridoma clones specific for pigeon cytochrome c. *Cell.* 30:141–152.
9. Samelson, L.E., and R.H. Schwartz. 1983. T cell clone-specific alloantisera that inhibit or stimulate antigen-induced T cell activation. *J. Immunol.* 131:2645–2650.
10. White, J., A. Pullen, K. Choi, P. Marrack, and J.W. Kappler. 1993. Antigen recognition properties of mutant $V\beta3^+$ T cell receptors are consistent with an immunoglobulin-like structure for the receptor. *J. Exp. Med.* 177:119–125.
11. Berg, L.J., B. Fazekas de St. Groth, F. Ivars, C.C. Goodnow, S. Gilfillan, H.J. Garchon, and M.M. Davis. 1988. Expression of T-cell receptor alpha-chain genes in transgenic mice. *Mol. Cell. Biol.* 8:5459–5469.
12. Berg, L.J., A.M. Pullen, B. Fazekas de St. Groth, D. Mathis, C. Benoist, and M.M. Davis. 1989. Antigen/MHC-specific T cells are preferentially exported from the thymus in the presence of their MHC ligand. *Cell.* 58:1035–1046.
13. Kaye, J., M.L. Hsu, M.E. Sauron, S.C. Jameson, N.R. Gascoigne, and S.M. Hedrick. 1989. Selective development of CD4+ T cells in transgenic mice expressing a class II MHC-restricted antigen receptor. *Nature.* 341:746–749.
14. Vasquez, N.J., J. Kaye, and S.M. Hedrick. 1992. In vivo and in vitro clonal deletion of double-positive thymocytes. *J. Exp. Med.* 175:1307–1316.
15. van Ewijk, W., Y. Ron, J. Monaco, J. Kappler, P. Marrack, M. Le Meur, P. Gerlinger, B. Durand, C. Benoist, and D. Mathis. 1988. Compartmentalization of MHC class II gene expression in transgenic mice. *Cell.* 53:357–370.
16. Bill, J., and E. Palmer. 1989. Positive selection of CD4+ T cells mediated by MHC class II-bearing stromal cell in the thymic cortex. *Nature.* 341:649–651.
17. Fink, P.J., L.A. Matis, D.L. McElligott, M. Bookman, and S.M. Hedrick. 1986. Correlations between T-cell specificity and the structure of the antigen receptor. *Nature.* 321:219–226.
18. Fink, P.J., L.A. Matis, S.B. Sorger, and S.M. Hedrick. 1988. The structure of the T cell receptor for antigen is correlated with T cell specificity. *Year Immunol.* 3:62–79.
19. Kaye, J., N.J. Vasquez, and S.M. Hedrick. 1992. Involvement of the same region of the T cell antigen receptor in thymic selection and foreign peptide recognition. *J. Immunol.* 148: 3342–3353.
20. Jorgensen, J.L., U. Esser, B. Fazekas de St. Groth, P.A. Reay, and M.M. Davis. 1992. Mapping T-cell receptor-peptide contacts by variant peptide immunization of single-chain transgenics. *Nature.* 355:224–230.
21. Ehrich, E.W., B. Devaux, E.P. Rock, J.L. Jorgensen, M.M. Davis, and Y.H. Chien. 1993. T cell receptor interaction with peptide/major histocompatibility complex (MHC) and superantigen/MHC ligands is dominated by antigen. *J. Exp. Med.* 178:713–722.
22. Lamont, A.G., A. Sette, and H.M. Grey. 1990. Inhibition of antigen presentation in vitro and in vivo by MHC antagonist peptides. *Int. Rev. Immunol.* 6:49–59.
23. Spain, L.M., J.L. Jorgensen, M.M. Davis, and L.J. Berg. 1994. A peptide antigen antagonist prevents the differentiation of T cell receptor transgenic thymocytes. *J. Immunol.* 152:1709–1717.
24. Lyons, D.S., S.A. Lieberman, J. Hampl, J.J. Boniface, Y. Chien, L.J. Berg, and M.M. Davis. 1996. A TCR binds to antagonist ligands with lower affinities and faster dissociation rates than to agonists. *Immunity.* 5:53–61.
25. Kozono, H., J. White, J. Clements, P. Marrack, and J. Kappler. 1994. Production of soluble MHC class II proteins with covalently bound single peptides. *Nature.* 369:151–154.
26. Kozono, H., D. Parker, J. White, P. Marrack, and J. Kappler. 1995. Multiple binding sites for bacterial superantigens on soluble class II MHC molecules. *Immunity.* 3:187–196.
27. Liu, C.P., D. Parker, J. Kappler, and P. Marrack. 1997. Selection of antigen-specific T cells by a single IEk peptide combination. *J. Exp. Med.* 186:1441–1450.
28. Otwinowski, Z., and W. Minor. 1997. Processing of X-ray diffraction data dollected in oscillation mode. *In* Macromolecular Crystallography Part A. C.W.J. Carter, and R.M. Sweet, editors. Academic Press Inc., Orlando, FL. 307–326.
29. CCP4. 1994. The CCP4 suite: programs for protein crystal-

lography. *Acta Crystallogr. D. Biol. Crystallogr.* 50:760–763.
30. Navaraza, J. 1994. AMoRe: an automated package for molecular replacement. *Acta Crystallogr. A. Biol. Crystallogr.* 50: 157–163.
31. Fremont, D.H., W.A. Hendrickson, P. Marrack, and J. Kappler. 1996. Structures of an MHC class II molecule with covalently bound single peptides. *Science.* 272:1001–1004.
32. Brunger, A.T., P.D. Adams, G.M. Clore, W.L. DeLano, P. Gros, R.W. Grosse-Kunstleve, J.S. Jiang, J. Kuszewski, M. Nilges, N.S. Pannu, et al. 1998. Crystallography and NMR system: a new software suite for macromolecular structure determination. *Acta Crystallogr. D Biol. Crystallogr.* 54:905–921.
33. Jones, T.A., and M. Kjeldgaard. 1997. Electron-density map interpretation. *Methods Enzymol.* 277:173–207.
34. Kleywegt, G.J., and T.A. Jones. 1996. xdlMAPMAN and xdlDATAMAN - programs for reformatting, analysis and manipulation of biomacromolecular electron-density maps and reflection data sets. *Acta Crystallogr. D.* 52:826–828.
35. Kleywegt, G.J., J.Y. Zou, M. Kjeldgaard, and T.A. Jones. 2001. Around O. *In* International Tables for Crystallography, Volume F. Crystallography of Biological Macromolecules. M.G. Rossmann and E. Arnold, editors. Dordrecht: Kluwer Academic Publishers, The Netherlands. 353–367.
36. Kersh, G.J., M.J. Miley, C.A. Nelson, A. Grakoui, S. Horvath, D.L. Donermeyer, J. Kappler, P.M. Allen, and D.H. Fremont. 2001. Structural and functional consequences of altering a peptide MHC anchor residue. *J. Immunol.* 166:3345–3354.
37. Evavold, B.D., and P.M. Allen. 1992. Dissection of the Hb(64–76) determinant reveals that the T cell receptor may have the capacity to differentially signal. *Adv. Exp. Med. Biol.* 323:17–21.
38. Marrack, P., L. Ignatowicz, J.W. Kappler, J. Boymel, and J.H. Freed. 1993. Comparison of peptides bound to spleen and thymus class II. *J. Exp. Med.* 178:2173–2183.
39. Buus, S., A. Sette, S.M. Colon, C. Miles, and H.M. Grey. 1987. The relation between major histocompatibility complex (MHC) restriction and the capacity of Ia to bind immunogenic peptides. *Science.* 235:1353–1358.
40. Livingstone, A.M., and C.G. Fathman. 1987. The structure of T-cell epitopes. *Annu. Rev. Immunol.* 5:477–501.
41. Finnegan, A., M.A. Smith, J.A. Smith, J. Berzofsky, D.H. Sachs, and R.J. Hodes. 1986. The T cell repertoire for recognition of a phylogenetically distant protein antigen. Peptide specificity and MHC restriction of staphylococcal nuclease-specific T cell clones. *J. Exp. Med.* 164:897–910.
42. Safley, S.A., P.E. Jensen, P.A. Reay, and H.K. Ziegler. 1995. Mechanisms of T cell epitope immunodominance analyzed in murine listeriosis. *J. Immunol.* 155:4355–4366.
43. Smith, C.A., C.M. Graham, and D.B. Thomas. 1994. Productive re-arrangement at both alleles of the T-cell receptor beta-chain locus in CD4 T-cell clones specific for influenza haemagglutinin. *Immunology.* 81:502–506.
44. Cease, K.B., H. Margalit, J.L. Cornette, S.D. Putney, W.G. Robey, C. Ouyang, H.Z. Streicher, P.J. Fischinger, R.C. Gallo, C. DeLisi, et al. 1987. Helper T-cell antigenic site identification in the acquired immunodeficiency syndrome virus gp120 envelope protein and induction of immunity in mice to the native protein using a 16-residue synthetic peptide. *Proc. Natl. Acad. Sci. USA.* 84:4249–4253.
45. Schild, H., U. Gruneberg, G. Pougialis, H.J. Wallny, W. Keilholz, S. Stevanovic, and H.G. Rammensee. 1995. Natural ligand motifs of H-2E molecules are allele specific and illustrate homology to HLA-DR molecules. *Int. Immunol.* 7:1957–1965.
46. Guex, N., and M.C. Peitsch. 1997. SWISS-MODEL and the Swiss-PdbViewer: an environment for comparative protein modeling. *Electrophoresis.* 18:2714–2723.
47. Fremont, D.H., M. Matsumura, E.A. Stura, P.A. Peterson, and I.A. Wilson. 1992. Crystal structures of two viral peptides in complex with murine MHC class I H-2Kb. *Science.* 257:919–927.
48. Madden, D.R., D.N. Garboczi, and D.C. Wiley. 1993. The antigenic identity of peptide-MHC complexes: a comparison of the conformations of five viral peptides presented by HLA-A2. *Cell.* 75:693–708.
49. Stern, L.J., J.H. Brown, T.S. Jardetzky, J.C. Gorga, R.G. Urban, J.L. Strominger, and D.C. Wiley. 1994. Crystal structure of the human class II MHC protein HLA-DR1 complexed with an influenza virus peptide. *Nature.* 368:215–221.
50. Scott, C.A., P.A. Peterson, L. Teyton, and I.A. Wilson. 1998. Crystal structures of two I-Ad-peptide complexes reveal that high affinity can be achieved without large anchor residues. *Immunity.* 8:319–329.
51. Fremont, D.H., D. Monnaie, C.A. Nelson, W.A. Hendrickson, and E.R. Unanue. 1998. Crystal structure of I-Ak in complex with a dominant epitope of lysozyme. *Immunity.* 8:305–317.
52. Latek, R.R., A. Suri, S.J. Petzold, C.A. Nelson, O. Kanagawa, E.R. Unanue, and D.H. Fremont. 2000. Structural basis of peptide binding and presentation by the type I diabetes-associated MHC class II molecule of NOD mice. *Immunity.* 12:699–710.
53. Lee, K.H., K.W. Wucherpfennig, and D.C. Wiley. 2001. Structure of a human insulin peptide-HLA-DQ8 complex and susceptibility to type 1 diabetes. *Nat. Immunol.* 2:501–507.
54. Rabinowitz, J.D., C. Beeson, C. Wulfing, K. Tate, P.M. Allen, M.M. Davis, and H.M. McConnell. 1996. Altered T cell receptor ligands trigger a subset of early T cell signals. *Immunity.* 5:125–135.
55. Driscoll, P.C., J.D. Altman, J.J. Boniface, K. Sakaguchi, P.A. Reay, J.G. Omichinski, E. Appella, and M.M. Davis. 1993. Two-dimensional nuclear magnetic resonance analysis of a labeled peptide bound to a class II major histocompatibility complex molecule. *J. Mol. Biol.* 232:342–350.
56. Brown, J.H., T. Jardetzky, M.A. Saper, B. Samraoui, P.J. Bjorkman, and D.C. Wiley. 1988. A hypothetical model of the foreign antigen binding site of class II histocompatibility molecules. *Nature.* 332:845–850.
57. Gahm, S.J., B.J. Fowlkes, S.C. Jameson, N.R. Gascoigne, M.M. Cotterman, O. Kanagawa, R.H. Schwartz, and L.A. Matis. 1991. Profound alteration in an alpha beta T-cell antigen receptor repertoire due to polymorphism in the first complementarity-determining region of the beta chain. *Proc. Natl. Acad. Sci. USA.* 88:10267–10271.
58. Garcia, K.C., M. Degano, R.L. Stanfield, A. Brunmark, M.R. Jackson, P.A. Peterson, L. Teyton, and I.A. Wilson. 1996. An alphabeta T cell receptor structure at 2.5 A and its orientation in the TCR-MHC complex. *Science.* 274:209–219.
59. Garboczi, D.N., P. Ghosh, U. Utz, Q.R. Fan, W.E. Biddison, and D.C. Wiley. 1996. Structure of the complex between human T-cell receptor, viral peptide and HLA-A2. *Nature.* 384:134–141.

60. Wilson, I.A., and K.C. Garcia. 1997. T-cell receptor structure and TCR complexes. *Curr. Opin. Struct. Biol.* 7:839–848.
61. Reinherz, E.L., K. Tan, L. Tang, P. Kern, J. Liu, Y. Xiong, R.E. Hussey, A. Smolyar, B. Hare, R. Zhang, et al. 1999. The crystal structure of a T cell receptor in complex with peptide and MHC class II. *Science.* 286:1913–1921.
62. Hennecke, J., A. Carfi, and D.C. Wiley. 2000. Structure of a covalently stabilized complex of a human alphabeta T-cell receptor, influenza HA peptide and MHC class II molecule, HLA-DR1. *EMBO J.* 19:5611–5624.
63. Reiser, J.B., C. Darnault, A. Guimezanes, C. Gregoire, T. Mosser, A.M. Schmitt-Verhulst, J.C. Fontecilla-Camps, B. Malissen, D. Housset, and G. Mazza. 2000. Crystal structure of a T cell receptor bound to an allogeneic MHC molecule. *Nat. Immunol.* 1:291–297.
64. Lamb, J.R., D.D. Eckels, P. Lake, J.N. Woody, and N. Green. 1982. Human T-cell clones recognize chemically synthesized peptides of influenza haemagglutinin. *Nature.* 300:66–69.
65. Kaye, J., S. Porcelli, J. Tite, B. Jones, and C.A. Janeway, Jr. 1983. Both a monoclonal antibody and antisera specific for determinants unique to individual cloned helper T cell lines can substitute for antigen and antigen-presenting cells in the activation of T cells. *J. Exp. Med.* 158:836–856.